

LETTERS

Early evolution of the venom system in lizards and snakes

Bryan G. Fry^{1,2}, Nicolas Vidal^{3,4}, Janette A. Norman², Freek J. Vonk⁵, Holger Scheib^{6,7}, S. F. Ryan Ramjan¹, Sanjaya Kuruppu⁸, Kim Fung⁹, S. Blair Hedges³, Michael K. Richardson⁵, Wayne C. Hodgson⁸, Vera Ignjatovic^{10,11}, Robyn Summerhayes^{10,11} & Elazar Kochva¹²

Among extant reptiles only two lineages are known to have evolved venom delivery systems, the advanced snakes and helodermatid lizards (*Gila Monster* and *Beaded Lizard*)¹. Evolution of the venom system is thought to underlie the impressive radiation of the advanced snakes (2,500 of 3,000 snake species)^{2–5}. In contrast, the lizard venom system is thought to be restricted to just two species and to have evolved independently from the snake venom system¹. Here we report the presence of venom toxins in two additional lizard lineages (*Monitor Lizards* and *Iguania*) and show that all lineages possessing toxin-secreting oral glands form a clade, demonstrating a single early origin of the venom system in lizards and snakes. Construction of gland complementary-DNA libraries and phylogenetic analysis of transcripts revealed that nine toxin types are shared between lizards and snakes. Toxinological analyses of venom components from the Lace Monitor *Varanus varius* showed potent effects on blood pressure and clotting ability, bioactivities associated with a rapid loss of consciousness and extensive bleeding in prey. The iguanian lizard *Pogona barbata* retains characteristics of the ancestral venom system, namely serial, lobular non-compound venom-secreting glands on both the upper and lower jaws, whereas the advanced snakes and anguimorph lizards (including *Monitor Lizards*, *Gila Monster* and *Beaded Lizard*) have more derived venom systems characterized by the loss of the mandibular (lower) or maxillary (upper) glands. Demonstration that the snakes, iguanians and anguimorphs form a single clade provides overwhelming support for a single, early origin of the venom system in lizards and snakes. These results provide new insights into the evolution of the venom system in squamate reptiles and open new avenues for biomedical research and drug design using hitherto unexplored venom proteins.

In helodermatid lizards, venom is made by a gland on the lower jaw from which ducts lead onto grooved teeth along the length of the mandible¹. In contrast, snake venom is produced by specialized glands in the upper jaw^{1,6–12} and is a shared derived trait of the advanced snakes^{2–5,13}. To investigate the evolution of venomous function in squamates we first obtained sequence data from five nuclear protein-coding genes representing major squamate lineages. Our phylogenetic analyses show that the closest relatives of snakes are the anguimorph (which include the venomous helodermatids) and iguanian lizards (Fig. 1, and Supplementary Fig. 1). These results

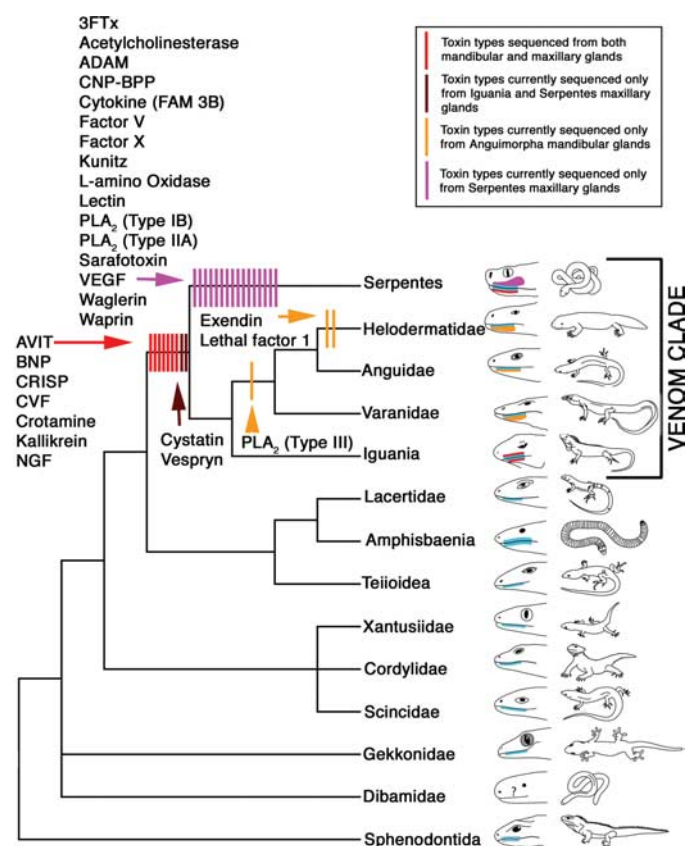


Figure 1 | Relative glandular development and timing of toxin recruitment events mapped over the squamate reptile phylogeny. Mucus-secreting glands are coloured blue; the ancestral form of the protein-secreting gland (serial, lobular and non-compound) red; of the complex, derived form of the upper snake-venom gland (compound, encapsulated and with a lumen) fuchsia, and the complex, derived form of the anguimorph mandibular venom gland (compound, encapsulated and with a lumen) orange. 3FTx, three-finger toxins; ADAM, a disintegrin and metalloproteinase; CNP-BPP, C-type natriuretic peptide-bradykinin-potentiating peptide; CVP, cobra venom factor; NGF, nerve growth factor; VEGF, vascular endothelial growth factor.

¹Australian Venom Research Unit, Level 8, School of Medicine, University of Melbourne, Parkville, Victoria 3010, Australia. ²Population and Evolutionary Genetics Unit, Museum Victoria, GPO Box 666E, Melbourne, Victoria 3001, Australia. ³Department of Biology and Astrobiology Research Center, 208 Mueller Lab, Pennsylvania State University, University Park, Pennsylvania 16802-5301, USA. ⁴UMS 602, Taxonomie et collections, Reptiles-Amphibiens, Département Systématique et Évolution, Muséum National d'Histoire Naturelle, 25 Rue Cuvier, Paris 75005, France. ⁵Institute of Biology, Leiden University, Kaiserstraat 63, PO Box 9516, 2300 RA, Leiden, The Netherlands. ⁶Department of Structural Biology and Bioinformatics, University of Geneva and Swiss Institute of Bioinformatics, Centre Médical Universitaire, 1 Rue Michel-Servet, 1211 Geneva 4, Switzerland. ⁷SBC Lab AG, Seebühlstrasse 26, 8185 Winkel, Switzerland. ⁸Monash Venom Group, Department of Pharmacology, Monash University, Clayton, Victoria 3800, Australia. ⁹Molecular and Health Technologies, CSIRO, 343 Royal Parade, Parkville, Victoria 3010, Australia. ¹⁰Department of Pathology, University of Melbourne, Parkville, Victoria 3010, Australia. ¹¹Murdoch Children's Research Institute, Royal Children's Hospital, Flemington Road, Parkville, Victoria 3052, Australia. ¹²Department of Zoology, Tel Aviv University, Tel Aviv 69978, Israel.

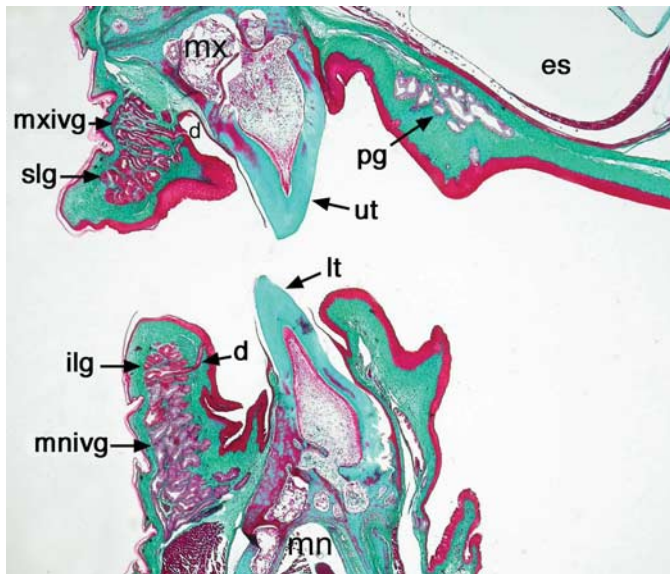


Figure 2 | Transverse section of *Pogona barbata* (Eastern Bearded Dragon) head to show relative arrangement of glands. Stain: Masson's trichrome. Original magnification $\times 40$. Abbreviations: d, duct; es, eye socket; ilg, infralabial gland; lt, lower tooth; mn, mandible; mnivg, mandibular incipient venom gland; mx, maxillary; mxivg, maxillary incipient venom gland; pg, palatine gland; slg, supralabial gland; ut, upper tooth.

represent a major paradigm shift in the understanding of squamate evolution. The three lineages were previously considered as part of a large, unresolved polytomy that also included amphisbaenian, lacertid and teioid lizards^{14,15}. We subsequently mapped the structure of protein-secreting oral glands (mandibular and maxillary) over our revised squamate phylogeny (Fig. 1). The anguimorphs,

iguanians and snakes, which form a well-resolved clade, are shown to be the only lineages possessing protein-secreting mandibular and/or maxillary glands. The presence of a protein-secreting gland is therefore a shared derived trait of this entire clade. The basal condition of a serial, lobular and non-compound protein-secreting gland, present in both mandibular and maxillary regions, is retained in the iguanian lizards (Fig. 2). The restriction of protein-secreting function to the maxillary (advanced snakes) or mandibular (anguimorphs) glands represents highly derived conditions. In the respective regions, the snakes (maxillary) and anguimorphs (mandibular) have independently evolved complex, compound venom glands with encapsulation and lumen formation for the storage of liquid venom for ready delivery^{1,16,17}. Some snakes (for example *Natrix*) still express proteins in their serial, lobular, non-compound mandibular glands, whereas the anguimorphs have lost the maxillary glands entirely¹⁸.

To explain the distribution, recruitment¹⁹ and molecular evolution²⁰ of venom proteins among them, representatives of the anguimorph/iguanian/serpent clade, spanning a wide ecological breadth, were also investigated for the secretion of toxins through the construction of cDNA libraries. Mandibular gland cDNA libraries were constructed for the Eastern Bearded Dragon (an iguanian) and four varanids (anguimorphs); maxillary-gland cDNA libraries were also constructed for the Eastern Bearded Dragon. To provide greater coverage of venom evolution, maxillary-gland cDNA libraries were also constructed from seven advanced snake families. Transcripts coding for previously characterized lizard or snake toxin types were identified in all gland cDNA libraries and we report the presence of venom toxins in lizards (other than *Heloderma*). Nine toxin types were recovered from both lizard and snake cDNA libraries (AVIT, B-type natriuretic peptide (BNP), CRISP, cobra venom factor, crotamine, cystatin, kallikrein, nerve growth factor and vespryn), being secreted from mandibular and maxillary glands. Bayesian phylogenetic analyses^{13,19} of these nine toxin types resulted in the monophyly of each venom toxin to the

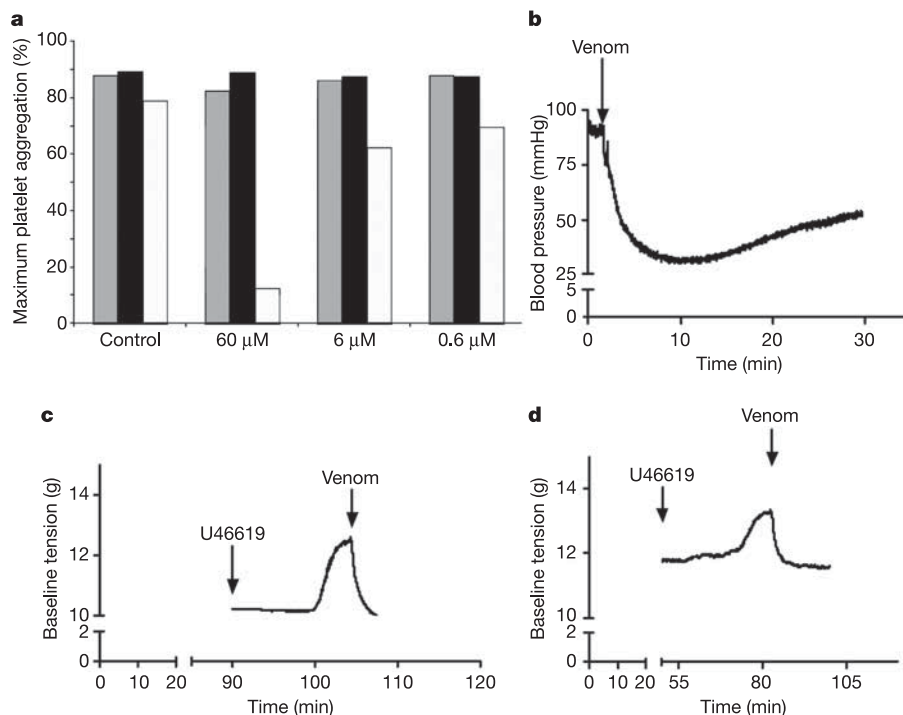


Figure 3 | Bioactivity of *V. varius* (Lace Monitor) venom. **a**, The effect of different molar concentrations of purified type III PLA₂ toxin DQ139930 on platelet aggregation. The control was saline. Grey bars, 2 μ M ADP; black bars, 30 μ M adrenaline; white bars, 5 μ M adrenaline. **b**, Effect of intravenous

injection of crude venom (1 mg kg⁻¹) on blood pressure in the anaesthetized rat. **c, d**, Effect of crude venom (200 μ g ml⁻¹) on U46619 precontracted endothelium-intact (**c**) and endothelium-denuded (**d**) aortic rings. $n = 3$; single traces are shown.

exclusion of related non-venom proteins. This pattern strongly supports single early recruitment events¹³ for each toxin type before the separation of snakes, iguanians and anguimorphs (Supplementary Figs 2–10). An additional toxin, type III phospholipase A₂ (PLA₂), previously characterized only from *Heloderma* venoms²¹ (Gila Monster and Beaded Lizard), was identified in varanid mandibular glands.

The mapping of toxin types, revealed in this study as being secreted in both mandibular and maxillary glands, over the revised squamate phylogeny provides additional insights into the evolution of the reptile venom chemical arsenal (Fig. 1). Most striking is the proposed complexity of the venom secretions in the common ancestor of venomous lizards and snakes with nine toxin types present. Seven of these were previously known only from snake venoms, including one toxin type (crotonamine), sequenced from the Eastern Bearded Dragon mandibular and maxillary glands, previously characterized only from rattlesnake venoms. The nine shared venom toxins isolated all possess previously well-characterized activities, including hypolocomotion, hypotension, hypothermia, immunomodulatory effects, intestinal cramping, myonecrosis, paralysis of peripheral smooth muscle unregulated activation of the complement cascade, and hyperalgesia¹⁹. The type III PLA₂ toxins from *Heloderma* venoms have been shown to block platelet aggregation²¹. Some of these toxins have been shown to have potent systemic effects, such as the profound hypotension produced by kallikrein and natriuretic toxins¹⁹ leading to rapid loss of consciousness, or coagulation disorders such as prolonged bleeding as a consequence of the *Heloderma* type III PLA₂ toxins²¹. Some toxins exert effects that, although non-lethal, may aid in the rapid incapacitation of prey items or potential predators, such as the markedly increased sensitivity to pain (hyperalgesia) and strong cramping produced by the AVIT toxins¹⁹.

Varanid venom was revealed by toxinological analyses to be as complex and potent as previously analysed reptile venoms^{5,22}. Liquid chromatography/mass spectrometry⁵ (LC/MS) showed the varanid

secretions to be rich in proteins with molecular masses consistent with the following toxin types sequenced from varanid cDNA libraries: natriuretic (2–4 kDa), type III PLA₂ (about 15 kDa), CRISP (23–25 kDa) and kallikrein (23–25 kDa) (Supplementary Fig. 11). Haematological assays of varanid type III PLA₂ toxin (DQ139930) purified by reverse-phase high-performance liquid chromatography²³ showed inhibition of platelet aggregation (Fig. 3a). Consistent with the same bioactivity as *Heloderma* type III PLA₂ (ref. 21) was the preservation of cysteines and cysteine spacing as well as the conservation of functional residues (Supplementary Fig. 12A). As cDNA sequencing and LC/MS analysis indicated a high concentration of kallikrein and BNP-type natriuretic toxins in the varanid secretions, additional assays investigated hypotension-inducing bioactivity. Intravenous injections of crude *Varanus varius* mandibular secretion to anaesthetized rats rapidly produced a sharp drop in blood pressure (Fig. 3b) and specific analyses with precontracted rat aortic rings²³ demonstrated the natriuretic peptide action of relaxation of aortic smooth muscle (Fig. 3c, d). Consistent with the preserved bioactivity of the varanid BNP-type natriuretic toxins, sequence analysis and molecular modelling revealed the retention of residues necessary for natriuretic activity²³ (Fig. 4, and Supplementary Fig. 10). The varanid forms of the kallikrein toxins also show conservation of functional residues and cysteine spacing (Supplementary Fig. 12B). In the CRISP toxins, the varanid forms all have the loop I doublet (KR) that has been proposed to be an essential part of the blockage of cyclic-nucleotide-gated calcium channels (Supplementary Fig. 13). Most varanid CRISP isoforms also have the loop I motif (EXXF) thought to contribute to the inhibition of smooth muscle contraction through the blockage of L-type Ca²⁺ channels (Supplementary Fig. 13). Other toxin types vary to differing degrees in the relative conservation of molecular characteristics.

The combined cDNA, LC/MS, molecular modelling and pharmacological results are consistent with effects reported for varanid bites,

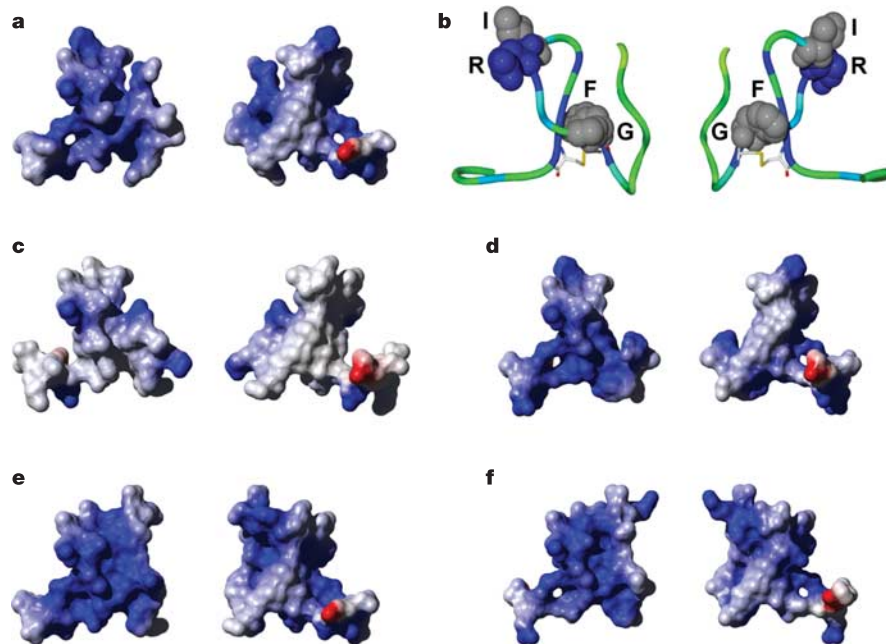


Figure 4 | Comparative modelling of representative natriuretic peptides. **a**, GNP-1 (DQ139927) from *V. varius* (Lace Monitor); **c**, TNP-c (P83230) from *Oxyuranus microlepidotus* (Inland Taipan); **d**, DNP (P28374) from *Dendroaspis angusticeps* (Eastern Green Mamba); **e**, Lebetin (Q7LZ09) from *Macrovipera lebetina* (Elephant Snake); **f**, BNP from the rat (P13205) brain and atria. Blue surface areas indicate positive charges, red areas show negative charges. Model pairs show the sides of the protein rotated by 180°.

b, GNP in ribbon representation coloured by alignment diversity²⁹. Conserved positions are in blue, brighter colours indicate increasing degree of variation. Functional residues²³ are CPK (Corey–Pauling–Koltun) coloured by amino-acid type²⁹. Hydrophobic residues are in grey, arginine in blue. The conserved cysteines are shown as sticks. To minimize confusion, all sequences are referred to by their SWISS-PROT accession numbers (<http://www.expasy.org/cgi-bin/sprot-search-ful>).

which include severe pain, breathing difficulties, skeletal muscle weakness and tachycardia²⁴. One of the authors (B.G.F.) has also acted as consultant on three varanid bites by captive bred specimens (*Varanus komodoensis* (Komodo Dragon), *V. scalaris* (Spotted Tree Monitor) and *V. varius* (Lace Monitor)), each of which resulted in rapid swelling (noticeable within minutes), dizziness, localized disruption of blood clotting and shooting pain extending from the affected digit up to the elbow, with some symptoms lasting for several hours. The rapidity and pathology are consistent with bioactive secretions rather than bacterial infection. In addition, varanid venom also has been shown to have the ability to rapidly paralyse small animals such as birds²⁵.

As well as providing evidence about the role of bioactive secretions in the effects produced by varanid bites, the complex and bioactive secretions present in 'non-venomous' lizards forces a fundamental rethinking of the very concept of 'non-venomous' reptile. The evolution of venomous function is considered to be a key innovation driving ecological diversification in advanced snakes²⁻⁵. Our results indicate that the single origin of venom in squamate reptiles might also have been a key factor in the adaptive radiation and subsequent ecological success of lizard lineages such as anguimorphs and iguanians; the well-supported anguimorph/iguanian/serpent clade represents about 4,600 out of about 7,900 extant squamate species, or 58% of the total squamate species diversity. There is also palaeontological evidence for the presence of venom delivery systems in some Upper Cretaceous anguimorphs and snakes^{8,26,27}. Because fossil data indicate that the clade containing anguimorphs, iguanians and snakes dates from Late Triassic/Early Jurassic²⁸, we infer that the venomous function arose once in squamate evolution, at about 200 Myr ago. This considerably revises previous estimates of about 100 Myr ago based on the assumed independent origin of venomous function in snakes and lizards.

Additional work aimed to investigate this special area of reptile evolution would include investigating the mandibular or maxillary secretions of all main lineages belonging to the toxin-secreting clade. Studies of additional transcriptomes may reveal earlier recruitment of a particular toxin type, such as those currently sequenced only from snake venoms for example, or may discover previously unrecognized toxin types. Further pharmacological investigations may shed more light upon the bioactivities and the relative use in defence, in prey capture or in predigestion. Because increased complexity of the venom gland was shown in this study to be linked to additional toxin recruitment events (Fig. 1), future work should include an exploration of the relationship between glandular complexity and the relative toxicity of the venom. The new lizard venom toxins exhibit considerable sequence diversity consistent with the birth-and-death mode of protein evolution that has given rise to a wide diversity of bioactivities in snake venoms²⁰. These molecules represent a tremendous hitherto unexplored resource not only for understanding reptile evolution but also for use in drug design and development.

METHODS

Toxin molecular evolution. Specimen collection localities: *Azemiops feae* (Fea's Viper), Guizhou, China; *Enhydryis polylepis* (Macleay's Water Snake), Darwin, Northern Territory, Australia; *Dispholidus typus* (Boomslang), Uganda; *Oxyuranus microlepidotus* (Inland Taipan), progeny of captive specimens from Goydnor's Lagoon, South Australia; *Pogona barbata* (Eastern Bearded Dragon), progeny of Brisbane, Queensland, Australia locality captive specimens; *Telescopus dhara* (Egyptian Catsnake), Egypt; *Trimorphodon biscutatus* (Lye Snake), Arizona, USA; *Liophis poecilgyrus* (Gold-bellied Snake), Paraguay; *Leioheterodon madagascariensis* (Madagascar Giant Hognosed Snake), Madagascar; *Philodryas olfersii* (Argentine Racer), Argentina; *Rhabdophis tigrinus* (Tiger Keelback), Hunan, China; *Varanus acanthurus* (Spiny-tailed Monitor), progeny of captive specimens collected from Newman, Western Australia; *Varanus mitchelli* (Mitchell's Water Monitor), Kununurra, Western Australia; *Varanus panoptes rubidus* (Desert Spotted Goanna), Sandstone, Western Australia; *Varanus varius* (Lace Monitor), Mallacoota, Victoria, Australia.

RNA extraction and construction of cDNA library: these steps were undertaken with the Qiagen RNeasy and Oligotex messenger RNA kits and the Creator SMART cDNA Library Construction Kit from BD Biosciences. Full details are available in Supplementary Information.

Histology. Tissue was dissected from animals after killing, then fixed in Bouin's fluid and decalcified overnight in acid alcohol (5% HCl in 70% ethanol). The tissues were dehydrated in graded ethanols, cleared in HistoClear and embedded in paraffin. Sections were cut to 10 µm thickness and stained with Masson's trichrome (Goldner's modification), Alcian blue at pH 1.0 and 2.4 alone or counterstained with haematoxylin-eosin or periodic acid Schiff in accordance with standard techniques.

Molecular modelling. Three-dimensional models were generated by aligning target sequences to the 1Q01 template with SPDBV²⁹. Sequence-to-structure alignments were sent to the Swiss-Model server. For the resulting models a van der Waals surface was calculated in MolMol³⁰. Surfaces were coloured by a 'simplecharge' potential as calculated in MolMol.

Pharmacology. Male rats were anaesthetized with sodium pentobarbitone (60–100 mg kg⁻¹, intraperitoneally). Venom or vehicle (namely 0.1% BSA) was administered through the jugular-vein cannula. Blood pressure was measured with a Gould (P23) pressure transducer attached to a carotid artery cannula, and recorded on a MacLab system.

Platelet aggregometry. Blood samples were collected from normal, healthy adult volunteers ($n = 2$) who had not taken any medication during the week before collection. Whole-blood samples were mixed 9:1 with 0.106 M sodium citrate. Citrated blood samples were centrifuged for 10 min at 100 g at 20 °C. The supernatant platelet-rich plasma (PRP) was removed and rested at room temperature for 30 min before assay. Platelet-poor plasma (PPP) for each volunteer was also prepared (by centrifugation for 20 min at 3,500 g) for platelet aggregometry. Platelet aggregation was measured with the Aggram platelet aggregometer and Hemoram software (Helena Laboratories). PRP aliquots (225 µl) were incubated in glass cuvettes for 2 min at 37 °C. Purified *Varanus varius* PLA₂ toxin DQ139930 (60, 6 and 0.6 µM) was added to the PRP and incubated at 37 °C for 3 min before the addition of agonist (2 µM ADP, or 5 or 30 µM adrenaline), to induce platelet aggregation, or sterile saline as a control. Platelet aggregation was monitored for 10 min. The degree of maximum platelet aggregation was assessed by measuring the optical transmission of light, zeroed with the appropriate PPP for each patient sample, through the PRP samples and compared with the controls (PRP samples assayed without the addition of toxin).

Squamate reptile phylogeny. Recent studies^{14,15} included representatives of all major squamate lineages and identified a clade comprising the following five lineages: first, Scincoidea (Scincidae, Xantusiidae and Cordylidae); second, Teiioidea (Teiidae and Gymnophthalmidae), Lacertidae and Amphisbaenia (Rhineuridae, Bipedidae, Trogonophidae and Amphisbaenidae); third, Iguania (Iguanidae, Agamidae and Chamaeleontidae); fourth, Anguimorpha (*Varanidae*, *Helodermatidae*, *Anguinae*, *Shinisaurus* and *Xenosaurus*); and fifth, Serpentes. The venomous squamates (advanced snakes and helodermatid lizards) are included in this large clade, whereas two other families of squamates (Gekkonidae and Dibamidae) are excluded^{14,15}. We focused on this clade and sampled five nuclear protein-coding genes, including two genes (*C-mos* and *RAG1*) used in other studies and three genes (*RAG2*, *R35* and *HOXA13*) not used previously to clarify squamate phylogeny. Phylogenies were built with probabilistic approaches (maximum-likelihood (ML) and bayesian methods of inference). Because separate analyses showed no significant topological incongruence, we performed combined analyses, which are considered to be our best estimates of phylogeny. Scincoidea was used as the outgroup because it was shown to be the most basal lineage of the clade^{14,15}. The bayesian and ML trees obtained were identical and showed significant support for most nodes (see Supplementary Information). In particular, a clade that includes Serpentes, Iguania and Anguimorpha was resolved (bayesian posterior probability 100%; ML bootstrap value 99%). In turn, we found that the closest relative of this clade is one comprising Teiioidea, Lacertidae and Amphisbaenia. Full details are available in Supplementary Information.

Received 13 July; accepted 17 October 2005.

Published online 16 November 2005.

- Kochva, E. In *Biology of the Reptilia* Vol 8 (eds Gans, S. K. & Gans, C.) 43–162 (Academic, London, 1978).
- Vidal, N. Colubroid systematics: evidence for an early appearance of the venom apparatus followed by extensive evolutionary tinkering. *J. Toxicol. Toxin Rev.* 21, 21–41 (2002).
- Vidal, N. & Hedges, S. B. Higher-level relationships of caenophidian snakes inferred from four nuclear and mitochondrial genes. *C. R. Biol.* 325, 987–995 (2002).

4. Fry, B. G. *et al.* Isolation of a neurotoxin (alpha-cobrotoxin) from a 'non-venomous' colubrid: evidence for early origin of venom in snakes. *J. Mol. Evol.* **57**, 446–452 (2003).
5. Fry, B. G. *et al.* LC/MS (liquid chromatography, mass spectrometry) analysis of Colubroidea snake venoms: evolutionary and toxicological implications. *Rapid Commun. Mass Spectrom.* **17**, 2047–2062 (2003).
6. Kochva, E. Development of the venom gland and trigeminal muscles in *Vipera palaestinae*. *Acta Anat.* **52**, 49–89 (1963).
7. Kochva, E. The development of the venom gland in the opisthoglyph snake *Telescopus fallax* with remarks on *Thamnophis sirtalis* (Colubridae, Reptilia). *Copeia* **2**, 147–154 (1965).
8. Kochva, E. The origin of snakes and evolution of the venom apparatus. *Toxicon* **25**, 65–106 (1987).
9. Kochva, E. *Atractaspis* (Serpentes, Atractaspididae) the Burrowing Asp; a multidisciplinary minireview. *Bull. Nat. Hist. Mus. Lond. Zool.* **68**, 91–99 (2002).
10. Underwood, G. & Kochva, E. On the affinities of the burrowing asps *Atractaspis* (Serpentes: Atractaspididae). *Zool. J. Linn. Soc.* **107**, 3–64 (1993).
11. Underwood, G. in *Venomous Snakes: Ecology, Evolution and Snakebite* (eds Thorpe, R. S., Wüster, W. & Malhotra, A.) 1–13 (Symp. Zool. Soc. Lond. no. 70, Clarendon, Oxford, 1997).
12. Jackson, K. The evolution of venom-delivery systems in snakes. *Zool. J. Linn. Soc.* **137**, 337–354 (2003).
13. Fry, B. G. & Wüster, W. Assembling an arsenal: Origin and evolution of the snake venom proteome inferred from phylogenetic analysis of toxin sequences. *Mol. Biol. Evol.* **21**, 870–883 (2004).
14. Vidal, N. & Hedges, S. B. Molecular evidence for a terrestrial origin of snakes. *Proc. R. Soc. Lond. B Suppl.* **271**, S226–S229 (2004).
15. Townsend, T. M., Larson, A., Louis, E. & Macey, J. R. Molecular phylogenetics of Squamata: the position of snakes, Amphisbaenians, and Dibamids, and the root of the squamate tree. *Syst. Biol.* **53**, 735–757 (2004).
16. Gabe, M. & Saint Girons, H. Données histologiques sur les glandes salivaires des lépidosauriens. *Mém. Mus. Natl. Hist. Nat. Paris* **58**, 1–118 (1969).
17. Gabe, M. & Saint Girons, H. in *Toxins of Animal and Plant Origin* (eds de Vries, A. & Kochva, E.) 65–68 (Gordon & Breach, London, 1971).
18. Gygax, P. Entwicklung, Bau und Funktion der Giftdrüse (Duvernoy's gland) von *Natrix tessellata*. *Acta Trop. Zool.* **28**, 225–274 (1971).
19. Fry, B. G. From genome to 'venome': Molecular origin and evolution of the snake venom proteome inferred from phylogenetic analysis of toxin sequences and related body proteins. *Genome Res.* **15**, 403–420 (2005).
20. Fry, B. G. *et al.* Molecular evolution of elapid snake venom three finger toxins. *J. Mol. Evol.* **57**, 110–129 (2003).
21. Huang, T. F. & Chiang, H. S. Effect on human platelet aggregation of phospholipase A2 purified from *Heloderma horridum* (beaded lizard) venom. *Biochim. Biophys. Acta* **1211**, 61–68 (1994).
22. Fry, B. G. *et al.* Electrospray liquid chromatography/mass spectrometry fingerprinting of *Acanthophis* (death adder) venoms: taxonomic and toxicological implications. *Rapid Commun. Mass Spectrom.* **16**, 600–608 (2002).
23. Fry, B. G. *et al.* Novel natriuretic peptides from the venom of the inland taipan (*Oxyuranus microlepidotus*): Isolation, chemical and biological characterization. *Biochem. Biophys. Res. Commun.* **327**, 1011–1015 (2005).
24. Soviev, O., Makeev, B. M., Kudryavtsev, S. B. & Makarov, A. N. A case of intoxication by a bite of the gray monitor (*Varanus griseus*). *Izv. Akad. Nauk Turkm. SSR. Ser. Biol. Nauk* **87**, 78 (1987).
25. Gorelov, Y. U. K. About the toxicity of the saliva of the gray monitor. *Izv. Akad. Nauk Turkm. SSR. Ser. Biol. Nauk* **71**, 74 (1971).
26. Pregill, G. K., Gauthier, J. A. & Greene, H. W. The evolution of Helodermatid squamates, with description of a new taxon and an overview of Varanoidea. *Trans. San Diego Soc. Nat. Hist.* **21**, 167–202 (1986).
27. Norell, M. A., McKenna, M. C. & Novacek, M. J. *Estesia mongoliensis*, a new fossil varanoid from the Late Cretaceous Barun Goyot Formation of Mongolia. *Am. Mus. Novit.* **3045**, 1–24 (1992).
28. Evans, S. E. At the feet of the dinosaurs: the origin, evolution and early diversification of squamate reptiles (Lepidosauria: Diapsida). *Biol. Rev. Camb.* **78**, 513–551 (2003).
29. Guex, N. & Peitsch, M. C. SWISS-MODEL and the Swiss-PdbViewer: an environment for comparative protein modeling. *Electrophoresis* **18**, 2714–2723 (1997).
30. Koradi, R., Billeter, M. & Wuthrich, K. MOLMOL: a program for display and analysis of macromolecular structures. *J. Mol. Graph.* **14**(1M), 51–55 (1996).

Supplementary Information is linked to the online version of the paper at www.nature.com/nature.

Acknowledgements We thank the following persons and institutions who helped us or contributed tissue samples used in this study: A. Fry, Alice Springs Reptile Centre, Australian Reptile Park, M. A. G. de Bakker, R. L. Bezy, B. Branch, J. Campbell, N. Clemann, C. Clemente, C. Cicero, K. Daoues, A. S. Delmas, B. Demeter, J. Haberfield, A. Hassanin, Healesville Sanctuary, M. Hird, Louisiana State University Museum of Zoology, P. Moler, T. Moncuit, P. Moret, National Museum of Natural History Naturalis Leiden (J. W. Arntzen), T. Pappenfus, J.-C. Rage, C. Skliris, J. Smith, S. Sweet, Ultimate Reptiles (South Australia), University of California Museum of Vertebrate Zoology (Berkeley), J. Walker, R. Waters, J. Weigel and B. Wilson. We also thank A. Webb and T. Purcell for providing HPLC access; N. Williamson for help with preliminary mass spectrometry characterization; E. V. Grishin for help in obtaining the references in Russian; S. Edwards for comments; and T. van Wagner and V. Wexler for artwork. This work was funded by the Service de Systématique moléculaire of the Muséum National d'Histoire Naturelle, Institut de Systématique (N.V.) and by grants from the Australian Academy of Science (B.G.F.), Australian Geographic Society (B.G.F.), Australia & Pacific Science Foundation (B.G.F.), Australian Research Council (B.G.F.), CASS Foundation (B.G.F.), Commonwealth of Australia Department of Health and Aging (B.G.F.), Ian Potter Foundation (B.G.F.), International Human Frontiers Science Program Organisation (B.G.F.), Leiden University (F.J.V., M.K.R.), NASA Astrobiology Institute (S.B.H.), National Science Foundation (S.B.H.) and University of Melbourne (B.G.F.). We thank the relevant wildlife departments for granting the scientific permits for field collection of required specimens.

Author Information The sequences of the cDNA clones have been deposited in GenBank (accession numbers DQ139877–DQ139931 and DQ184481), as have the nuclear gene sequences (DQ119594–DQ119641). Reprints and permissions information is available at npg.nature.com/reprintsandpermissions. The authors declare no competing financial interests. Correspondence and requests for materials should be addressed to B.G.F. (bgf@unimelb.edu.au).